DOI: 10.21062/mft.2024.090 http://www.journalmt.com

Advancing the Ductile Behaviour of Heavy-Wall API X70 Pipeline Steel by a "Slab/Sheet" Thickness Ratio Increase

Vadym Zurnadzhy (0000-0003-0290-257X)[1,2], Yuliia Chabak (0000-0003-3743-7428)[1,2], Ivan Petryshynets (0000-0001-8001-5349)[2], Alexey Efremenko (0000-0001-7670-0423)[1], Ivan Sili (0000-0002-6603-2174)[1], Ruslan Sagirov (0000-0003-3575-8324)[3], Vasily Efremenko (0000-0002-4537-6939)[1,2]
[1]Pryazovskyi State Technical University. Gogolya 29, 49044 Dnipro. Ukraine. E-mail: vzurnadzhy@saske.sk, juliachabak25@gmail.com, sili_i_i@pstu.edu, alexeyefr@gmail.com, vgefremenko@gmail.com
[2]Institute of Materials Research, Slovak Academy of Sciences. Watsonova 47, 040 01 Kosice. Slovak Republic. E-mail: ipetryshynets@saske.sk
[3]Metallurgical Plant Kametstal. Soborna 18B, 51900 Kamians'ke. Ukraine. E-mail: r.i.sagirov@gmail.com

The present work was aimed at studying the effect of a "Slab/Sheet" thickness ratio (SSTR) on the microstructure and mechanical properties of API 5L X70 steel sheets intended for heavy-wall oil/gas pipelines. The 25 mm-thick and 40 mm-thick steel sheets were rolled from the cast slabs of different thicknesses (250 mm and 300 mm) and their mechanical properties were compared. The sheets were subjected to thermo-mechanical controlled processing followed by accelerating cooling, resulting in the structure of quasi-polygonal/acicular ferrite with minor amounts of granular pearlite and martensite-austenite constituents. Increasing the cast slab thickness significantly improved the ductility and low-temperature impact toughness of steel sheets regardless of their thickness. Specifically, a total elongation increased by 3-6 points (up to 26-28 %); an absorbed impact energy (tested at –20 °C) – in 1.5-1.8 times (up to 300-370 J); the DWTT shear area (at –20 °C) – in 1.6-2.1 times (up to 81-91.7 %). The properties advancement under SSTR increase was associated with an additional refinement of ferrite grains and better homogenization of cast structure under deeper hot deformation.

Keywords: X70 steel sheet, Slab thickness, TMCP, accelerated cooling, Mechanical properties, DWTT

1 Introduction

High-strength rolled steel is one of the most important structural materials used in different engineering applications, including oil/gas production and transportation [1-3]. The pipelines are produced of steel sheets manufactured according to the API 5L X60-X80 grades specifications [4, 5]. The optimization of its production route and further improvement of mechanical properties are the priority tasks of the metallurgical industry. Steel sheets of the above grades should perform an improved combination of strength, ductility, and impact toughness as well as they should be easily welded in field conditions (the deterioration of their mechanical properties in the heat-affected zone is also a matter of concern [6, 7]). Thereby, X60-X80 grades pipeline steel is subjected to thermo-mechanical controlled processing (TMCP) where the finish rolling temperature (FRT) and the reduction ratio (thickness decrease) in the last rolling passes are strictly monitored [8-10]. TMCP is often followed by accelerating cooling (AC) (using the water flows) in a special unit settled just after the rolling mill [11-13]. The TMCP/AC technology considerably enhances the strength and low-temperature impact toughness of the steel addressing the requirements of higher API 5L grade (X70, X80) [14-16]. It is important that TMCP/AC is a cost-saving processing that does not include the additional furnace heating for heat treatment (in contrast to the operations of normalization or quenching/tempering which can also be applied under the production of the high-strength structural steels [17,18]).

It is well-known that the mechanical properties of rolled steel are crucially affected by the "Slab/Sheet" thickness ratio (SSTR) which shows the maximum reduction ratio under deformation. Thus, SSTR predetermines how the cast dendritic structure and segregation zones will be eliminated in the cast billet during its hot rolling [19]. With the reduction ratio increase, the steel sheets become more uniform in chemical composition and structure, especially in an axial zone, leading to higher ductility and impact toughness [20, 21]. To control the latter, Charpy V-notch test (CVNT) and the drop weight tear test (DWTT) at subzero temperature (–20 °C and lower) are applied [22, 23]. The slabs of 200-270 mm thickness are widely used to produce X70 grade steel [24]. With an increase in the sheet's thickness, the deformation in the axial zone becomes more constrained, which promotes brittle fracture

propagation [25]. For this reason (constrained deformation), ensuring the required DWTT results (at least 85% of a shear area [25]) in the thick sheets is a challenging task [26]. Therefore, for the heavy-wall (≥20 mm thick) pipelines, an increase in the structure homogeneity and a decrease in cross-sectional segregation are vital for the mechanical properties, especially for the low-temperature steel toughness.

In a view of above, the cast slabs of at least 300 mm in thickness are applied for the manufacturing of the heavy-wall sheets [27] providing a deeper working out of metal due to higher SSTR [28, 29]. However, using the thick slabs implies correcting the rolling process parameters (on both the rough and finish stages) since it may affect the structure formation processes (phase transformation, the recrystallization kinetics, carbide precipitation. etc.) thus deteriorating the resultant structure and mechanical properties. Accordingly, the regimes of accelerated cooling should be adjusted also to provide the required structure distribution in a sheet's cross-section [30, 31]. The effect of manufacturing parameters on the properties of API 5L X70 pipeline steel is repeatedly studied in many works [32-34]. However, there are still a limited number of studies dedicated to the structure and mechanical performance of the thick steel sheets of an X70 grade depending on a "Slab/Sheets" thickness ratio. The object of the present work was to evaluate the feasibility of using the 300 mm thick steel slabs to produce the heavy-wall (25-40 mm) sheets meeting the requirements of X70 grade and paying special attention to the low-temperature behaviour under the impact loading.

2 Materials and Methods

The experimental material was rolled steel sheets of API 5L X70 grade of the following chemical composition (in wt.%): 0.08 C, 1.60 Mn, 0.26 Si, 0.10 Cr, 0.06 Mo, 0.28 Ni, 0.045 Nb, 0.045 V, 0.14 Cu, 0.02 Cr, 0.002 S, 0.010 P and Fe – balance. Steel was produced by the oxygen converter process and continuously cast into the slabs of conventional thickness (250 mm, denoted as slab A) and of increased thickness (300 mm, slab B). The slabs were used to produce the sheets 6000 mm long and 2000 mm wide with different thicknesses of 25 mm and 40 mm, applying the TMCP/AC technology. The values of a "Slab/Sheet" thickness ratio were as follows: (a) 10.0 (slab A) and 12.0 (slab B) – for 25-mm thick sheet; (b) 6.3 (slab A) and 7.5 (slab B) – for 40 mm-thick sheet.

After heating to 1180-1200 °C (with a soaking for 5.5 hours) slabs were rolled according to the following procedure: (a) the rough rolling (reduction of the slabs to 135-140 mm at 1040-1060 °C), (b) intermediate rolling (reduction to 100-112 mm at 910-930 °C), (c) finish rolling with starting in a γFe interval below the non-recrystallization temperature (T_{nr}); the last passes were performed close to Ar_3 temperature pursuing the grain refinement and inheriting higher dislocation density. The above finish rolling parameters were selected based on the T_{nr} and Ar_3 temperatures calculation as follows [35]:

$$T_{nr}= 887+464C+(6445Nb - 644\sqrt{Nb})+(732V - 230\sqrt{V})+ 890Ti + 363Al - 357Si\ [^oC], \quad (1)$$

$$Ar_3=910 - 310C - 80Mn - 20Cu - 55Ni - 15Cr - 80Mo + 35Si\ [^oC], \quad (2)$$

Where:

C, Nb, V, Ti, Al, Mn, Cu, Ni, Cr, Mo, Si...The contents of chemical elements [wt.%].

The T_{nr} and Ar_3 values were calculated as 968.9 °C and 758.2 °C, respectively. Accordingly, the finish rolling started at ~840 °C and finished at ~760 °C. Afterward, the sheets were subjected to accelerating cooling by water starting from ~745 °C: the 25 mm-thick sheets were cooled to 550-570 °C, and the 40-mm thick sheets – to 470-500 °C (in both cases the cooling rate was ~20 °C/s). After the AC finished, the sheets were collected in a stack, where they slowly cooled in the air to 100 °C for 40 hours. A schematic sketch of TMCP/AC processing and its parameters are depicted in Fig.1.

The tensile/impact specimens were cut in a longitudinal direction at a depth of ¼ of thickness in accordance with APL 5L regulations. Tensile tests were performed in compliance with ISO 6892-1:2019, on cylindrical specimens with a gauge of 10 mm diameter, with a strain rate of 0.1 mm·s^{-1}. The V-notched specimens of 10×10×55 (mm) in size were used to measure absorbed impact energy under CVNT at –20 °C. DWTT was carried out at –20 °C on the full-thickness press-notched longitudinal-transversal specimens of 76×305×b (mm) in size (b stands for the sheet thickness). The results of DWTT were assessed by the fraction of shear (ductile) area (SA) on the rupture surface. The microstructure of the specimens was studied after polishing and etching by a 4 vol.% nital solution using the optical microscope (OM) "Axiovert 40 MAT" (Carl Zeiss). The scanning electron microscope (SEM) "JSM-7000F" (JEOL) was also employed to observe the microstructure and ruptured surface. The ferrite grain size and the structural banding degree were defined according to ASTM E112-19 and ASTM E1268-19 accordingly [36, 37]. The fine structure of the steel was investigated using the transmission electron microscopy (TEM)

"JEM-100-C-XII" (JEOL) (the TEM foils were mechanically polished to about 0.1 mm thickness, followed by fluid-jet electro-polishing in a 6-vol% solution of perchloric acid).

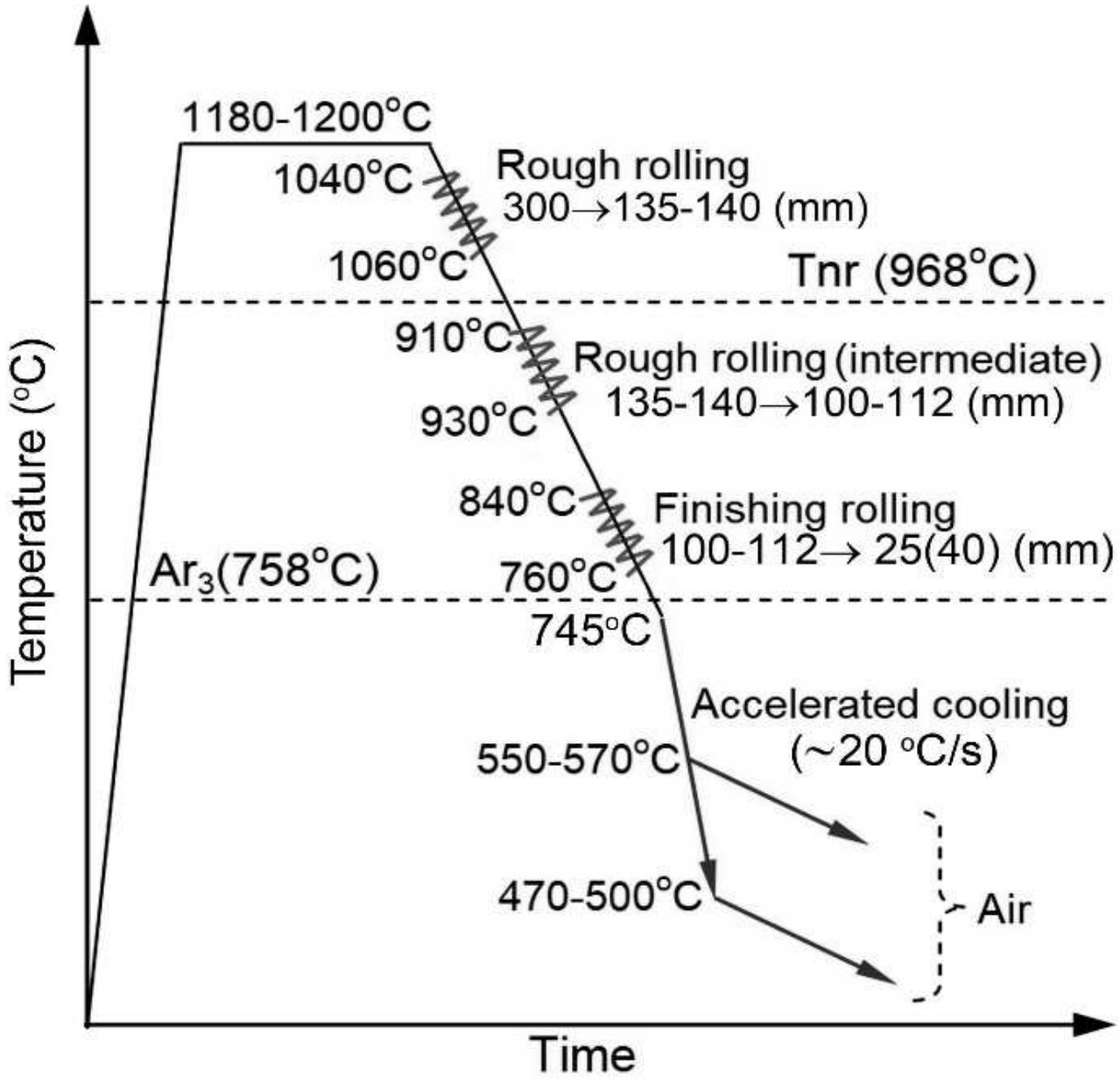

Fig. 1 *Schematic diagram of TMCP/AC processing in "Time-Temperature" coordinates*

3 Results and Discussion

Figure 2 presents the comparison of the mechanical properties of 25 mm-thick sheets produced from slabs of different thicknesses. After TMCP/AC, sheets made of slabs A and B showed almost the same average values of yield tensile strength (YTS) and ultimate tensile strength (UTS) (Fig. 2a), i.e., the increase in an SSTR did not affect the steel's strength. With that, the sheets made of slab B performed 1.5 times lower scatter of the experimental YTS and UTS values (shown by the dashed line) revealing more stable mechanical properties within the batch of sheets. As follows from Figs. 2b and 2c, with increasing slab thickness, the average total elongation (TEL) increased by 6 points (from 22 % to 28 % accounting for almost a one-third increase), while the average value of a low-temperature absorbed impact energy was almost doubled (from 205 J to 370 J). Moreover, in the latter case, the scatter of the experimental results decreased by 2.5 times. Regarding the DWTT, the sheets rolled from slab A exhibited a fairly large scatter of SA values (37-87%) with a mean value of 53% i.e., most of the sheets failed the API requirement on a low-temperature DWTT (SA ≥ 85%). On the contrary, the sheets produced of thicker slabs completely met with an X70 grade performing an average SA of 91.7% and a narrow scatter of the values (85-95 %).

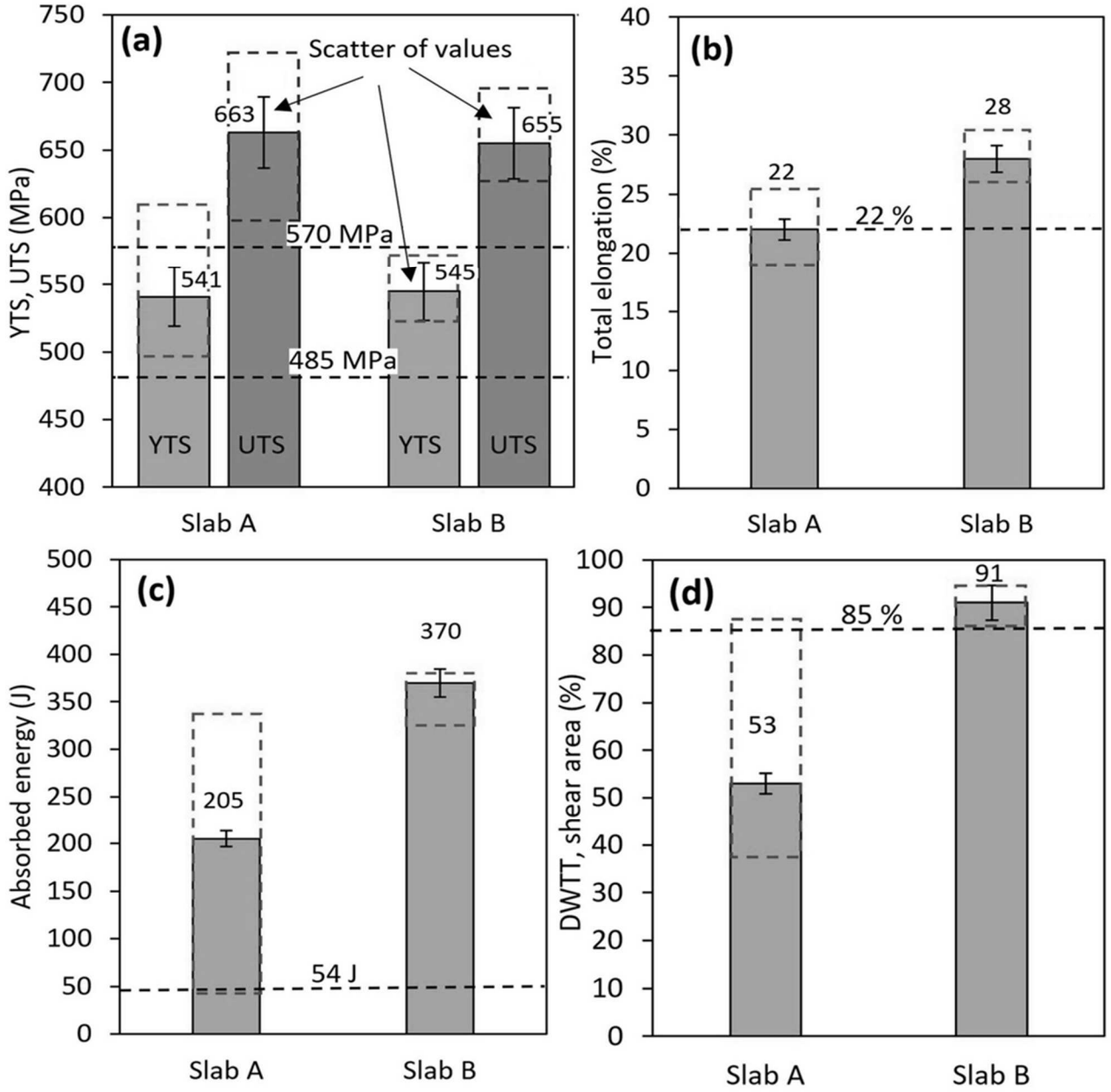

Fig. 2 *The mechanical properties of 25 mm-thick sheets produced from slabs of different thicknesses: (a) yield tensile strength and ultimate tensile strength, (b) total elongation, (c) absorbed impact energy (–20 °C), (d) the shear area (DWTT at –20 °C); The dashed black lines indicate the minimum thresholds of the properties according to API 5L X70 grade; The dashed red lines show the maximum scatter of the experimental results within the batch of sheets*

The mechanical properties of 40 mm-thick steel sheets are presented in Fig. 3. As seen in Fig. 3a, sheets made of slab B were somewhat inferior in terms of yield strength and tensile strength (on average by 9 MPa and 34 MPa, respectively), though they fully met the requirements of the X70 grade. In contrast, sheets of slab B exhibited higher (on average by 3 points) total elongation and 1.5 times higher absorbed impact energy. Noteworthy, the strength and ductility of the 40 mm-thick sheet were close to those of thinner (25 mm) sheets; this was obtained due to AC with a lower finish cooling temperature. In the context of absorbed energy, it can be concluded that the 40 mm-thick sheets were somewhat inferior to the 25 mm sheets. Moreover, in the case of a 40 mm-thick sheet, the advantage of slab B over slab A in the absorbed energy was lower than that of 25 mm thickness. This is attributed to lower SSTR increase (from 6.3 to 7.5) in the case of 40 mm-thick sheets, meaning less effective breakage of a cast dendritic/segregation pattern as compared to 25 mm-thick sheets. As follows from Fig. 3d, an increase in slab thickness positively affected DWTT results: the shear area increased on average from 37 % (sheets A) to 80% (sheets B) closely approaching to API required level.

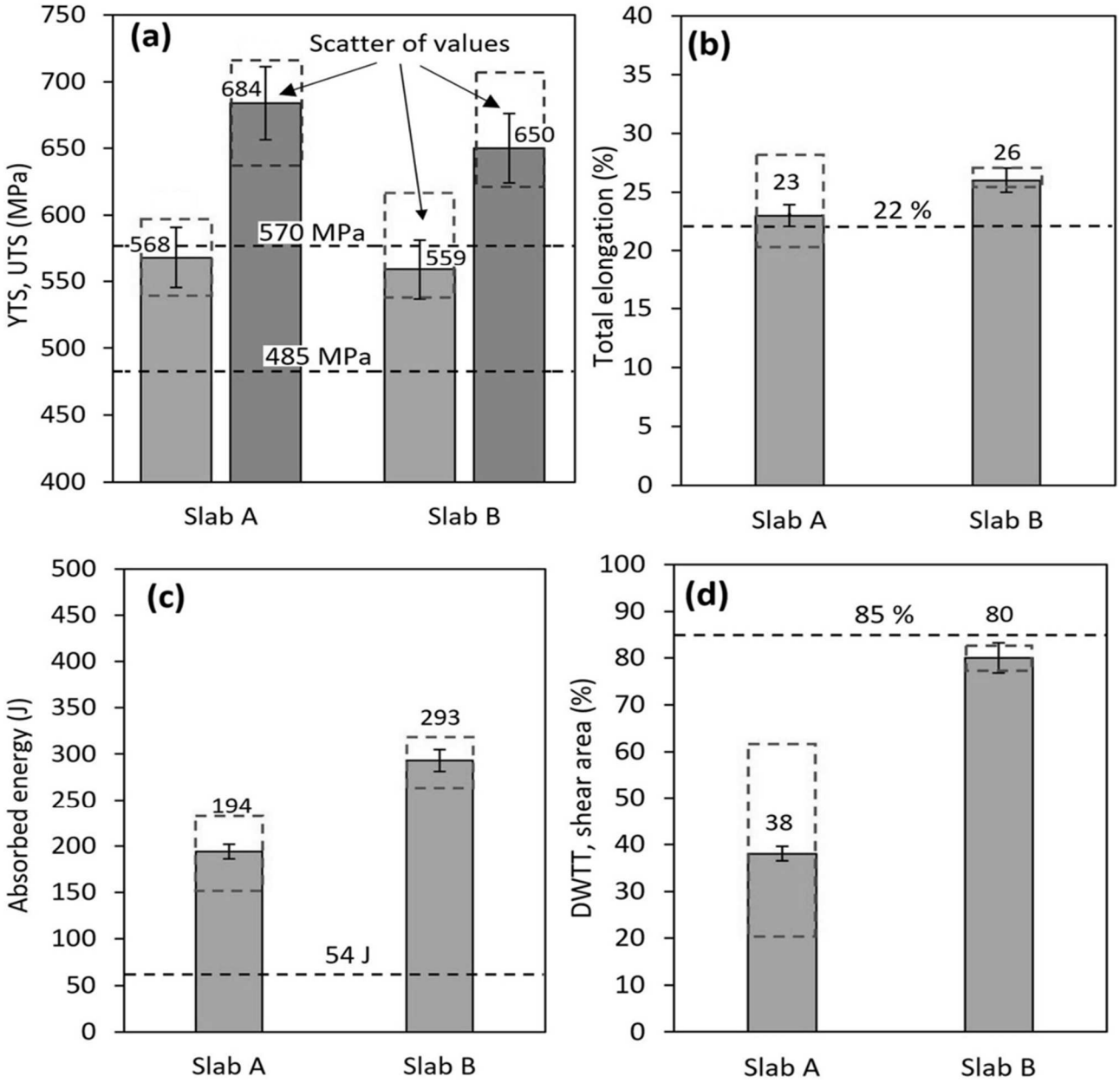

Fig. 3 *The mechanical properties of 40 mm-thick sheets produced from slabs of different thicknesses: a) yield tensile strength and ultimate tensile strength, (b) total elongation, (c) absorbed impact energy (–20 °C), (d) the shear area (DWTT at –20 °C); The dashed black lines indicate the minimum thresholds of the properties according to API 5L X70 grade; The dashed red lines show the maximum scatter of the experimental results within the batch of sheets*

The microstructure of the 25 mm-thick sheet rolled from slab B is shown in Fig. 4. When characterizing the thick steel sheet (of several tens of millimeters), it is important to evaluate the cross-sectional microstructure gradient from the subsurface layers to the axial zone (such gradient often appears due to cross-sectional variation in a plastic deformation degree under the hot rolling). According to API X70, the specimens for the mechanical properties testing should be cut from the layer at a ¼ of thickness depth. Meanwhile, the DWTT and exploitation behaviour of the sheet are dependent on the structure of the inner layers as well. Therefore, in this work, we studied the microstructure of the sheets at two levels: at a ¼ of thickness depth and in the axial zone. The "main" structure (at ¼-depth) consisted of a fine-grained quasi-polygonal and acicular ferrite (Fig. 4a). In this layer, the size of ferrite grains matched a grain number 11 (according to ASTM E112-13) meaning an average grain diameter of 7.9 μm. Also, the dispersed granular pearlite colonies and the martensite/austenite (M/A) islands were revealed in minor amounts. The presence of M/A constituents (shown by the arrows in Fig. 4b) is considered a positive factor contributing to the mechanical properties of steel [38, 39]. The appearance of M/A constituents is explained by austenite enrichment

with carbon under "austenite → ferrite" transformation [38] when the "austenite→pearlite" mechanism was inhibited due to alloying by Cr, Ni, Mo [40, 41] and accelerated cooling. The quasi-polygonal ferrite grains were divided by the high-angle boundaries (Fig. 4c) while they themselves had the inner cellular sub-structure with low-angle boundaries which acted as a barrier for the gliding dislocation [42] (Fig. 4d). Within the grains, the nano-sized precipitates of (Nb,V)C carbide were revealed interacting with dislocations by the Orowan mechanism (Fig. 4e) [43]. For comparison, Fig. 4f presents the microstructure of the axial zone which was consisted of quasi-polygonal fine-grained ferrite and short bainitic bands (the latter were associated with the segregation zones). Here, the ferrite grains were by 1 number (ASTM E112-13 [36]) coarser as compared with the layer at a ¼-depth. Thus, the differences in the structure across the 25 mm thick sheet section were insignificant. The structural banding (which could be evaluated according to ASTM E1268-19 [37]) was hardly revealed in the 25 mm sheet neither at a ¼-depth nor in an axial zone.

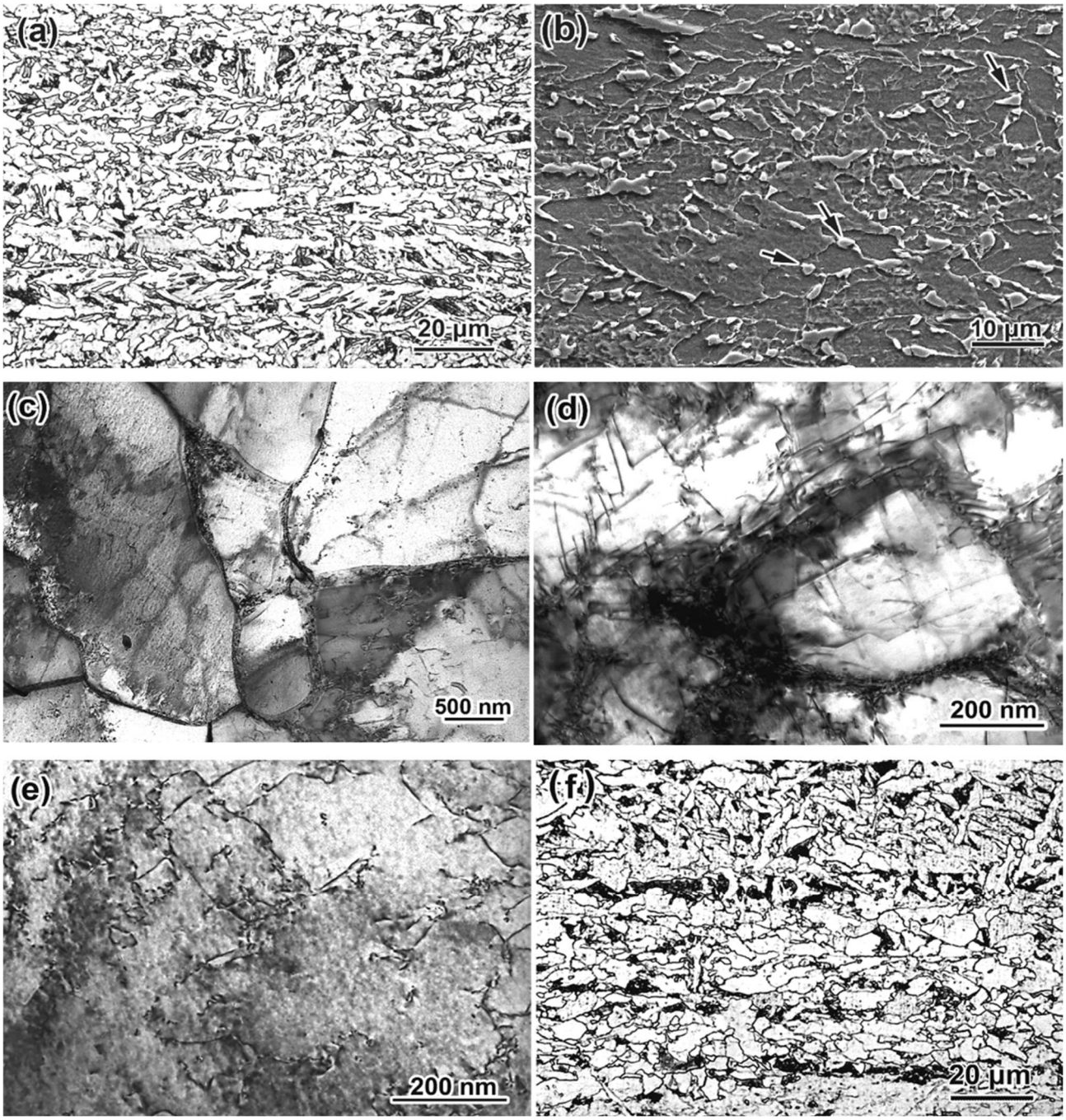

Fig. 4 *The microstructure of a 25 mm-thick sheet produced from a 300 mm-thick slab: a) a total view (OM), b) M/A constituents (SEM), c) high-angle grain boundaries (TEM), d) a cellular sub-structure (TEM), e) the precipitate/dislocation interaction (TEM), (f) at the axial zone of the sheet (OM); Images (a)-(e) refer to the depth of ¼ the sheet thickness*

Fig. 5 presents the microstructure of the 40 mm-thick sheet produced from slab B. At a depth of ¼ thickness, the microstructure (Fig. 5a) consisted of quasi-polygonal ferrite with a grain size corresponding to a number of 9-10 (ASTM E112-13) which is 11.2-15.9 μm in diameter on average. In the axial zone structure, consisted of a polygonal ferrite (with the grain size of number 9, Figs. 5b) and pearlite (Fig. 5c). In the sheet centre, ferritic grains had a more equiaxed (less elongated) shape compared to the ¼-depth; moreover, they did not acquire the pronounced cellular (sub-grained) pattern because of lower deformation in the axial zone (Fig. 5d). The structural banding in the 40 mm-thick sheets was estimated as of 1-2 degree mostly due to the discontinuous pearlite bands.

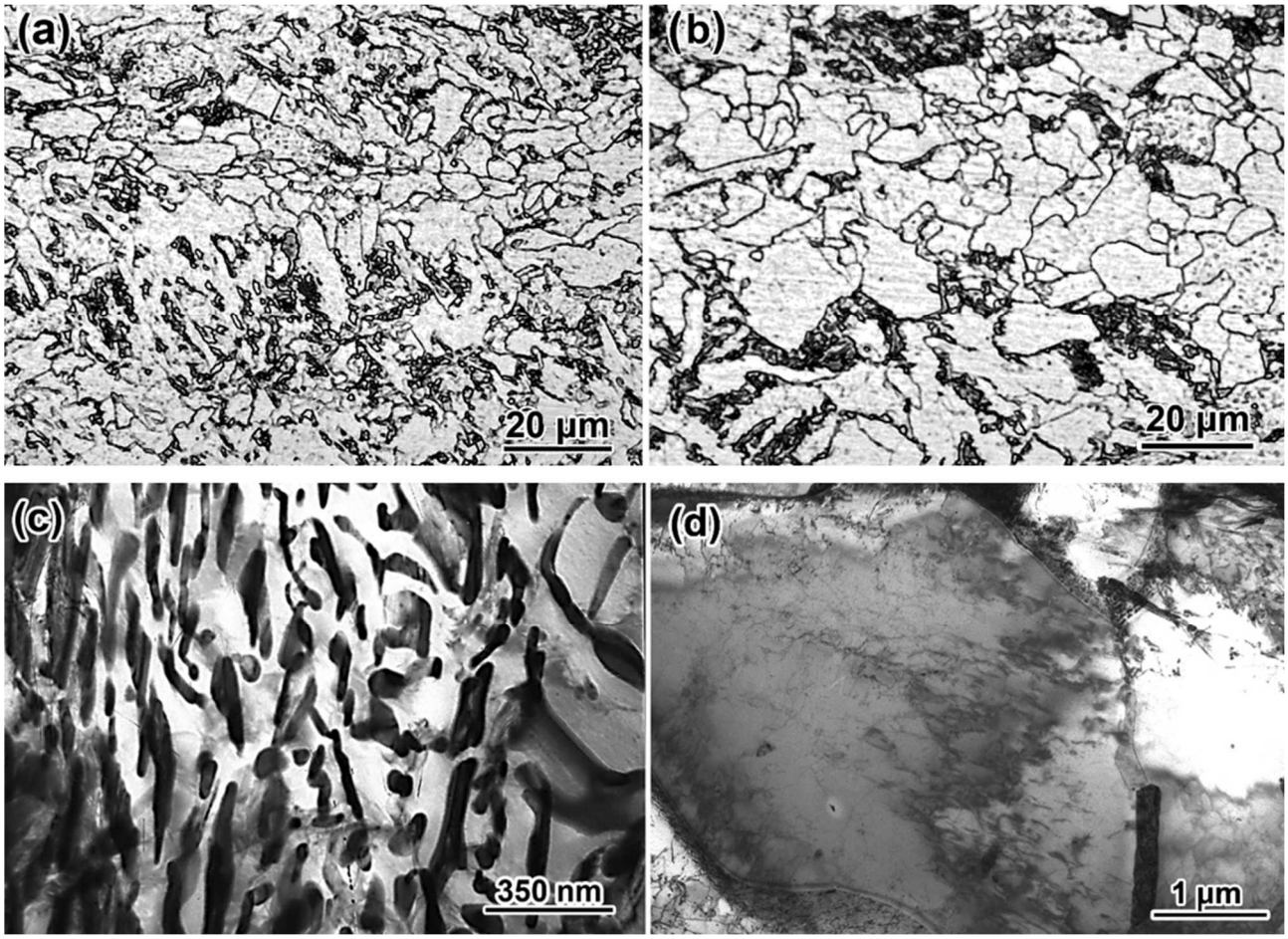

Fig. 5 *The microstructure of a 40 mm-thick sheet produced from a 300 mm-thick slab: (a) at a depth of ¼ the sheet thickness (OM), (b) in the axial zone of the sheet (OM), c) cementite carbides in pearlite colony (TEM), (d) ferrite grains in the axial zone of the sheet (TEM); Images (c) and (e) refer to the axial zone of the sheet*

The comparison of sheets made of slabs A and B shows a similar type of structure in both cases, while the thicker slabs ensured finer (by one-grain number) grain size. The grain refinement by using slab B is explained by a higher amount of rolling passes due to an increased slab thickness. Under each pass, austenite was subjected to deformation followed by recrystallization, which proceeded through the grain nucleation mechanism [44]. It can be assumed that the multiple nucleation might lead to gradual refinement of the initial (before the pass) austenite grain since its growth was inhibited given the continuous decrease in a sheet temperature from one pass to another. More uniform grain distribution over the sheet's cross-section is beneficial for pipeline applications where fatigue may occur [45, 46]. Furthermore, the SSTR increase means the greater thickness reduction, which resulted in better deterioration of the cast dendritic structure leading to higher structure/chemical homogeneity of steel. An increase in structural homogeneity is evidenced by a sharp decrease in the scatter of the results of mechanical properties testing, indicating higher result stability. This is an important aspect from the point of view of organizing product testing. Increasing the stability of results and obtaining the required properties during the first test allows to avoid the retesting or even additional heat treatment, which involves the extra costs of time and resources.

The results obtained show that increasing the slab thickness from 250 mm to 300 mm is beneficial for the mechanical performance of API X70 sheet steel intended for heavy-wall pipelines. This assertion is

confirmed by Fig. 6 depicting the enhancement of ductile/impact properties under the increase of SSTR: the total elongation, absorbed impact energy, and shear area (DWWT) were found to increase with an SSTR increase. Under the testing at –20 °C, the absorbed impact energy of 25 mm thick steel reached 300-370 J, which is 6-7 times to minimum level required by API 5L (Figs. 6a).

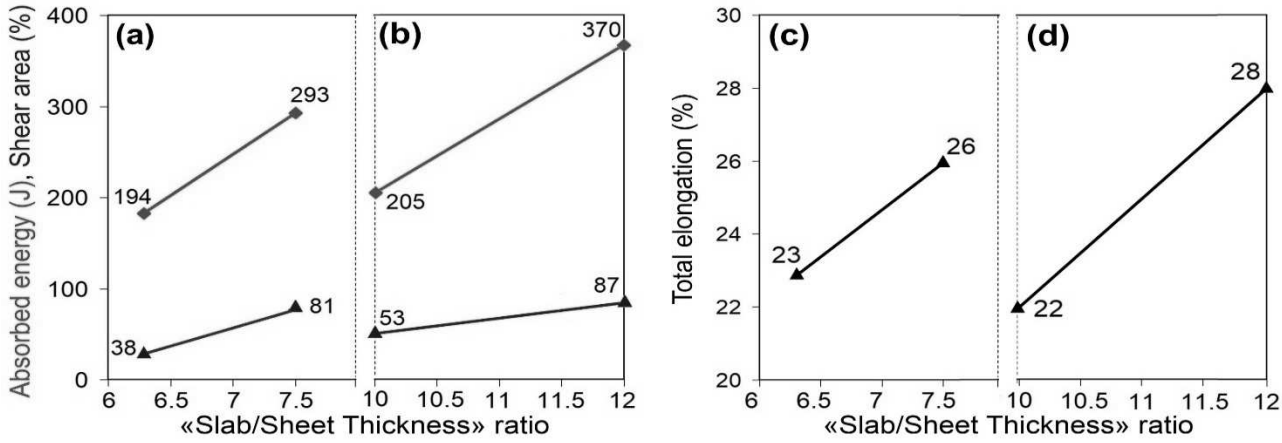

Fig. 6 *The effect of a "Slab/Sheet Thickness" ratio on mechanical properties of the X70 steel: (a) absorbed impact energy, shear area (DWTT), (b) total elongation. The numbers on the plot are the mean values of the mechanical properties*

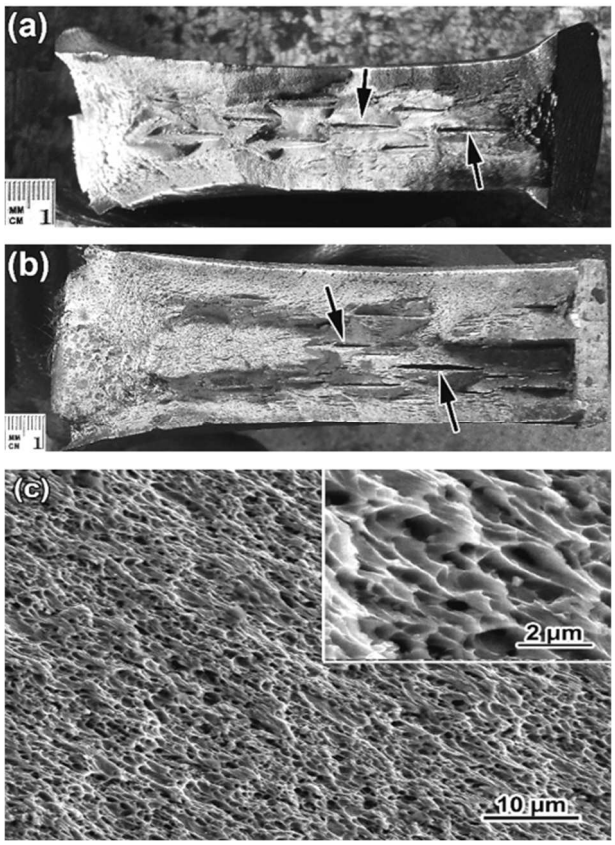

Fig. 7 *The fracture surface of DWTT specimens originating from slab B: (a) 25 mm-thick sheet (OM), (b) 40 mm-thick sheet (OM), (c) a fractured relief at the shear area in a 40 mm-thick DWTT specimen (SEM)*

The DWTT behaviour was also enhanced significantly by an SSTR increase (Fig. 6b). Figs. 7a and 7b illustrate the fractured DWTT specimens originating from slab B which present the ductile rupture for 25 mm and 40 mm sheets both. Notably, the separation (delamination) scars (shown by the arrows in Figs. 7a and 7b) are seen in both specimens, indicating an appropriate (ductile) mechanism of rupture [47-49]. According to Cho et al. [50], the separation creates a local free surface, thus inducing the formation of the elliptical shear lips that hinders the propagation of the cleavage fracture from the notch and provides the ductile fracture. The visual rupture characterization was supported by the SEM study of the shear area, which revealed multiple dimples on the surface of a 40 mm-thick DWTT specimen with no signs of cleavage pattern (Fig. 7c). While noting the positive effect of increasing the slab thickness on the steel's resistance to brittle fracture, it should be admitted that it does not affect the strength of the steel, which is determined mainly by the temperature-strain regimes of TMCP at the finish rolling stage and the parameters of accelerated cooling.

The present work has demonstrated the feasibility of using cast slabs of increased thickness to produce API 5L X70 grade steel sheets for heavy-wall pipelines. This allows increasing a "slab/sheet thickness" ratio, pursuing higher steel reduction for better homogenizing steel and refinement of its structure. As a result, the ductility and low-temperature impact toughness of steel can be significantly improved, which is important for safe pipeline exploitation.

4 Conclusions

The steel sheets for the heavy-wall oil/gas pipelines made of cast slabs of different thicknesses (250 mm and 300 mm) were comparatively investigated regarding microstructure and mechanical

properties considering their compliance with an API X70 grade. Using a thicker slab allows for an increase in the "Slab/Sheet" thickness ratio (SSTR). Accordingly, the effect of SSTR on the steel mechanical behaviour was evaluated in the present work. The main conclusions drawn are the following:

- When producing the 25 mm-thick and 40 mm-thick sheets of an API X70 grade subjected to the TMCP/AC treatment, an increase in SSTR from 10 to 12.0 and from 6.3 to 7.5, respectively, significantly enhanced the ductility and low-temperature impact toughness of steel sheets of both thicknesses. Specifically, the total elongation increased by 3-6 points (up to 26-28 %); absorbed impact energy (at –20 °C) – in 1.5-1.8 times (up to 300-370 J), and the shear area (DWTT at –20 °C) – in 1.6-2.1 times (up to 81.0-91.7 %).
- An advanced ductility of an API X70 steel under the SSTR increase refers to an additional refinement of ferrite grain and formation of cellular sub-grained pattern caused by higher slab reduction under hot rolling. Deeper deformation of a slab's cast structure resulted in the metal homogenization in terms of stability of the sheet mechanical properties (with several times a decrease in the scatter of the experimental results).
- The strength indicators (YTS, UTS) were not affected by the SSTR increase.
- In this research, it was confirmed that the "Slab/Sheet" thickness ratio is one of the key technological parameters that determine the mechanical properties of thick steel sheets and guarantee the reliable exploitation of heavy-wall pipelines in oil/gas transportation. Increasing SSTR to 7.5 and 12.0 due to the increase in slab thickness to 300 mm ensured compliance of the properties of 25 mm-thick and 40 mm-thick steel sheets with the requirements of API 5L X70 grade, including DWTT and subzero impact toughness, which is beneficial for low-temperature applications.

Acknowledgement

This work was funded by Ministry of Education and Science of Ukraine under the projects No. 0123U100374. The financial support in the framework of the Slovak Research and Development Agency project (APVV-23-0341) is greatly appreciated. Funded by the EU NextGenerationEU through the Recovery and Resilience Plan for Slovakia under the project No. 09I03-03-V01-00061 and No. 09I03-03-V01-00099.

References

[1] BRUSCHI, R., VITALI, L., MARCHIONNI, L., PARRELLA, A., MANCINI, A. (2015). Pipe technology and installation equipment for frontier deep water projects. In: *Ocean Engineering*, Vol. 108, pp. 369-392. https://doi.org/10.1016/j.oceaneng.2015.08.008

[2] KARNAUKH, S.G., MARKOV, O.E., KUKHAR, V.V., SHAPOVAL, A.A. (2022). Classification of steels according to their sensitivity to fracture using a synergetic model. In: *The International Journal of Advanced Manufacturing Technology*, Vol. 119, pp. 5277-5287. https://doi.org/10.1007/s00170-022-08653-y

[3] RYKAVETS, Z.M., BOUQUEREL, J., VOGT, J.-B., DURIAGINA, Z.A., KULYK, V.V., TEPLA, T.L., BOHUN, L.I., KOVBASYUK, T.M. (2019). Investigation of the microstructure and properties of TRIP 800 steel subjected to low-cycle fatigue. In: *Progress in Physics of Metals*, Vol. 20, pp. 620 – 633. https://doi.org/10.15407/ufm.20.04.620

[4] AZAM, M.A., SAFIE, N.E., HAMDAN, H.H. (2021). Effect of sulfur content in the crude oil to the corrosion behaviour of internal surface of API 5L X65 petroleum pipeline steel. In: *Manufacturing Technology*, Vol. 21(5), pp. 561-574. https://doi.org/10.21062/mft.2021.066

[5] LEE, S.I., LEE, S.Y., LEE, S.G., JUNG, H.G., HWANG, B. (2018). Effect of strain aging on tensile behavior and properties of API X60, X70, and X80 pipeline steels. In: *Metals and Materials International*, Vol. 24, pp. 1221-1231. https://doi.org/10.1007/s12540-018-0173-9

[6] LI, L., FU, J., WANG, X., LIU, K., NIU, X., LI, X., HAN, B. (2023). Comparative study of microstructure and toughness of automatic welded joints of X70 pipeline steel with no slope and 25 slope. In: *International Journal of Pressure Vessels and Piping*, Vol. 206, pp. 105054. https://doi.org/10.1016/j.ijpvp.2023.105054

[7] EFREMENKO, V.G., ZOTOV, D.S., ZURNADZHY, V.I., KUSSA, R.A.,

SAVENKO, V.I., SAGIROV, R.I., BOCHAROVA, O.A., EFREMENKO, A.V. (2021). Computer modelling-based selection of accelerated cooling parameters for advanced high-strength structural steel. In: *IOP Conf. Series: Materials Science and Engineering*, 1037, 012030. https://doi. org/10.1088/1757-899X/1037/1/012030

[8] MANDAL, G., GHOSH, S.K., CHATTERJEE, S. (2019). Effects of TMCP and QT on microstructure and properties of ultrahigh strength steel. In: *Materials Today: Proceedings*, Vol. 18, pp. 5196-5201. https://doi.org/10.1016/j.matpr.2019.07.519

[9] BUCHMAYR, B. (2017). Thermo-mechanical treatment of steels – a real disruptive technology since decades. In: *Steel Research International*, Vol. 88, pp. 1700182. https://doi.org/10.1002/srin.201700182

[10] NOWOTNIK, A., SIWECKI, T. (2010). The effect of TMCP parameters on the microstructure and mechanical properties of Ti-Nb microalloyed steel. In: *Journal of Microscopy*, Vol. 237, pp. 258-262. https://doi.org/10.1111/j.1365-2818.2009.03238.x

[11] ZHAO, W. HU, X. WANG, J. KANG, G. YUAN, DI, H., MISRA, R.D.K. (2016). Effect of microstructure on the crack propagation behavior of microalloyed 560MPa (X80) strip during ultra-fast cooling. In: *Materials Science and Engineering A*, Vol. 666, pp. 214-224. https://doi.org/10.1016/j.msea.2016.04.073

[12] EFREMENKO, V.G., POPOV, E.S., KUZ'MIN, S.O., TRUFANOVA, O.I., EFREMENKO, A.V. (2014). Introduction of three-stage thermal hardening technology for large diameter grinding balls. In: *Metallurgist*, Vol. 57, pp. 849 – 854. https://doi.org/10.1007/s11015-014-9812-7

[13] TANG, S., LIU, Z.Y., WANG, G.D., MISRA, R.D.K. (2013). Microstructural evolution and mechanical properties of high strength microalloyed steels: Ultra Fast Cooling (UFC) versus Accelerated Cooling (ACC). In: *Materials Science and Engineering: A*, Vol. 580, pp. 257-265. https://doi.org/10.1016/j.msea.2013.05.016

[14] SHIN, S.Y., WOO, K.J., HWANG, B., KIM, S., LEE, S. (2007). Analysis of fracture toughness in transition temperature region of API X70 and X80 linepipe steels. In: *Journal of Korean Institute of Metals and Materials*, Vol. 45, pp. 447-457.

[15] ZIDELMEL, S., KARIM, R., KAOUKA, A. (2024). Effects of thermo-mechanical parameters on microstructural and mechanical properties of API X70 steel. In: *The Journal of the Minerals, Metals & Materials Society*, pp. 1-8. https://doi.org/10.1007/s11837-023-06333-0

[16] WITEK, M. (2015). Possibilities of using X80, X100, X120 high-strength steels for onshore gas transmission pipelines. In: *Journal of Natural Gas Science and Engineering*, Vol. 27, pp. 374-384. https://doi.org/10.1016/j.jngse.2015.08.074

[17] GODEFROID, L.B., SENA, B.M., TRINDADE, V.B.D. (2017). Evaluation of microstructure and mechanical properties of seamless steel pipes API 5L type obtained by different processes of heat treatments. In: *Journal of Materials Research*, Vol. 20, pp. 514-522. https://doi.org/10.1590/1980-5373-MR-2016-0545

[18] ZURNADZHY, V.I., EFREMENKO, V.G., WU, K.M., PETRYSHYNETS, I., SHIMIZU, K., ZUSIN, A.M., BRYKOV, M.N., ANDILAKHAI, V.A. (2020). Tailoring strength/ductility combination in 2.5 wt% Si-alloyed middle carbon steel produced by the two-step Q-P treatment with a prolonged partitioning stage. In: *Materials Science and Engineering: A*, Vol. 791, pp. 139721. https://doi.org/10.1016/j.msea.2020.139721

[19] OMALE, J., OHAERI, E., RAHMAN, K.M.M., SZPUNAR, J., FATEH, F., ARAFIN, M. (2020). Through-thickness inhomogeneity of texture, microstructure, and mechanical properties after rough and finish rolling treatments in hot-rolled API 5L X70 pipeline steel. In: *Journal of Materials Engineering and Performance*, Vol. 29, pp. 8130-8144. https://doi.org/10.1007/s11665-020-05280-0

[20] HU, J., DU, L.X., XIE, H., GAO, X.H., MISRA, R.D.K. (2014). Microstructure and mechanical properties of TMCP heavy plate microalloyed steel. In: *Materials Science and Engineering: A*, Vol. 607, pp. 122-131. https://doi.org/10.1016/j.msea.2014.03.133
XU, L., QIAO, G., GONG, X., GU, Y., XU, K., XIAO, F. (2023). Effect of through-thickness microstructure inhomogeneity on mechanical properties and strain hardening behavior in heavy-wall X70 pipeline steels. In: *Journal of Materials Research and Technology*, Vol.

25, pp. 4216-4230. https://doi.org/10.1016/j.jmrt.2023.06.198G

[21] UO, F., WANG, X., LIU, W., SHANG, C., MISRA, R.D.K., WANG, H., PENG, C. (2018). The influence of centerline segregation on the mechanical performance and microstructure of X70 pipeline steel. In: *Steel Research International*, Vol. 89, pp. 1800407. https://doi.org/10.1002/srin.201800407

[22] TAGAWA, T., AMANO, T., HIRAIDE, T., SAKIMOTO, T., IGI, S., FUJISHIRO, T., TAKUYA, H., TAKEHIRO, I., AIHARA, S. (2018). Inverse fracture in DWTT and brittle crack behavior in large-scale brittle crack arrest test. In: *Journal of Pressure Vessel Technology*, Vol. 140, pp. 051205. https://doi.org/10.1115/1.4040641

[23] SAM, S., KANT, N., HAZRA, S.S. (2019). Development of API 5L X70 grade steel through thin slab casting and rolling process. In: *ASME 2019 India Oil and Gas Pipeline Conference*, Vol. 58530, pp. 293-299. https://doi.org/10.1115/IOGPC2019-4519

[24] SHIN, S.Y., HWANG, B., LEE, S., KIM, N.J., AHN, S.S. (2007). Correlation of microstructure and charpy impact properties in API X70 and X80 line-pipe steels. In: *Materials Science and Engineering: A*, Vol. 458, pp. 281-289. https://doi.org/10.1016/j.msea.2006.12.097

[25] HONG, S., SHIN, S.Y., LEE, S., KIM, N.J. (2011). Effects of specimen thickness and notch shape on fracture modes in the drop weight tear test of API X70 and X80 linepipe steels. In: *Metallurgical and Materials Transactions A*, Vol. 42, pp. 2619-2632. https://doi.org/10.1007/s11661-011-0697-9

[26] LI, H., GONG, M., LI, T., WANG, Z., WANG, G. (2020). Effects of hot-core heavy reduction rolling during continuous casting on microstructures and mechanical properties of hot-rolled plates. In: *Journal of Materials Processing Technology*, Vol. 283, pp. 116708. https://doi.org/10.1016/j.jmatprotec.2020.116708

[27] GOLI-OGLU, E.A., Efron, L.I., MOROZOV, Y.D. (2013). More effective thermo-mechanical treatment of microalloyed pipe steel. In: *Steel in Translation*, Vol. 43, pp. 113-119. https://doi.org/10.3103/S0967091213020101

[28] XU, Z., WANG, X., JIANG, M. (2017). Investigation on improvement of center porosity with heavy reduction in continuously cast thick slabs. In: *Steel Research International*, Vol. 88, pp. 1600061. https://doi.org/10.1002/srin.201600061

[29] OHAERI, E.G., SZPUNAR, J.A. (2022). An overview on pipeline steel development for cold climate applications. In: *Journal of Pipeline Science and Engineering*, Vol. 2, Issue 1, pp. 1-17. https://doi.org/10.1016/j.jpse.2022.01.003

[30] KOVAL', A.D., EFREMENKO, V.G., BRYKOV, M.N., ANDRUSHCHENKO, M.I., KULIKOVSKII, R.A., EFREMENKO, A.V. (2012). Principles for developing grinding media with increased wear resistance. Part 1. Abrasive wear resistance of iron-based alloys. In: *Journal of Friction and Wear*, Vol. 33, pp. 39-46. https://doi.org/10.3103/S1068366612010072

[31] YADAV, S., JACK, T.A., DAVANI, R.K.Z., OHAERI, E., SZPUNAR, J. (2022). Effect of post-processing heat treatment on hydrogen embrittlement susceptibility of API 5L X70 pipeline steel. In: *International Journal of Pressure Vessels and Piping*, Vol. 199, pp. 104762. https://doi.org/10.1016/j.ijpvp.2022.104762

[32] DAVANI, R.K.Z., OHAERI, E.G., YADAV, S., SZPUNAR, J.A., Su, J., GAUDET, M., RASHID, M., ARAFIN, M. (2024). Crystallographic texture and the mechanical properties of API 5L X70 pipeline steel designated for an arctic environment. In: *Materials Science and Engineering: A*, Vol. 889, pp. 145849. https://doi.org/10.1016/j.msea.2023.145849

[33] TURHAN, Ş.Ö., MOTAMENI, A., GÜRBÜZ, R. (2020). Fatigue behavior of welded API 5L X70 steel used in pipelines. In: *Journal of Failure Analysis and Prevention*, Vol. 20, pp. 1554-1567. https://doi.org/10.1007/s11668-020-00959-x

[34] KARJALAINEN, L.P., MACCAGNO, T.M., JONAS, J.J. (1995). Softening and flow stress behaviour of Nb microalloyed steels during hot rolling simulation. In: *ISIJ International*, Vol. 35, pp. 1523-1531. https://doi.org/10.2355/isijinternational.35.1523

[35] ASTM E112-13. Standard Test Methods for Determining Average Grain Size. ASTM International, West Conshocken, PA, 2021.

[36] ASTM E1268-19. Standard Practice for Assessing the Degree of Banding or Orientation of Microstructures. ASTM International, West Conshocken, PA, 2019.

[37] XIE, C., LIU, Z., HE, X., WANG, X., QIAO, S. (2020). Effect of martensite–austenite constituents on impact toughness of pre-tempered MnNiMo bainitic steel. In: *Materials Characterization*, Vol. 161, pp. 110139. https://doi.org/10.1016/j.matchar.2020.110139

[38] FAN, L., ZHOU, D., WANG, T., Li, S., WANG, Q. (2014). Tensile properties of an acicular ferrite and martensite/austenite constituent steel with varying cooling rate. In: *Materials Science and Engineering: A*, Vol. 590, pp. 224-231. https://doi.org/10.1016/j.msea.2013.10.037

[39] EFREMENKO, B.V., SHIMIZU, K., ESPALLARGAS, N., EFREMENKO, V.G., KUSUMOTO, K., CHABAK, Yu.G., BELIK, A.G., CHIGAREV, V.V., ZURNADZHY, V.I. (2020). High-temperature solid particle erosion of Cr-Ni-Fe-C arc cladded coatings. In: *Wear*, Vol. 460-461, pp. 203439. https://doi.org/10.1016/j.wear.2020.203439

[40] CHABAK, Y., EFREMENKO, B., PETRYSHYNETS, I., EFREMENKO, V., LEKATOU, A.G., ZURNADZHY, V., BOGOMOL, I., Fedun V., KOVAĽ K., Pastukhova T. (2021). Structural and tribological assessment of biomedical 316 stainless steel subjected to pulsed-plasma surface modification: comparison of LPBF 3D printing and conventional fabrication. In: *Materials*, Vol. 14, pp. 7671. https://doi.org/10.3390/ma14247671

[41] PAN H., He Y., ZHANG X. (2021). Interactions between dislocations and boundaries during deformation. In: *Materials*. Vol. 14(4), pp. 1012. https://doi.org/10.3390/ma14041012

[42] EFREMENKO, V.G., CHABAK, YU.G., FEDUN, V.I., SHIMIZU, K., PASTUKHOVA, T.V., PETRYSHYNETS, I., ZUSIN, A.M., KUDINOVA, E.V., EFREMENKO, B.V. (2021). Formation mechanism, microstructural features and dry-sliding behaviour of "Bronze/WC carbide" composite synthesised by atmospheric pulsed-plasma deposition. In: *Vacuum*, Vol. 185, 110031. https://doi.org/10.1016/j.vacuum.2020.110031

[43] ALANEME, K.K., OKOTETE, E.A. (2019). Recrystallization mechanisms and microstructure development in emerging metallic materials: A review. In: *Journal of Science: Advanced Materials and Devices*, Vol. 4, pp. 19-33. https://doi.org/10.1016/j.jsamd.2018.12.007.

[44] GIORGETTI, V., SANTOS, E.A., MARCOMINI, J.B., SORDI, V.L. (2019). Stress corrosion cracking and fatigue crack growth of an API 5L X70 welded joint in an ethanol environment. In: *International Journal of Pressure Vessels and Piping*, Vol. 169, pp. 223-229. https://doi.org/10.1016/j.ijpvp.2019.01.006

[45] OSTASH, O.P., KULYK, V.V., POZNYAKOV, V.D., GAIVORONS'KYI, O.A., VIRA, V.V. (2019). Influence of the modes of heat treatment on the strength and cyclic crack-growth resistance of 65G steel. In: *Materials Science*, Vol. 54, pp. 776-782. https://doi.org/10.1007/s11003-019-00263-6

[46] SUNG, H.K., SOHN, S.S., SHIN, S.Y., LEE, S., KIM, N.J., CHON, S.H., YOO, J.Y. (2012). Effects of finish rolling temperature on inverse fracture occurring during drop weight tear test of API X80 pipeline steels. In: *Materials Science and Engineering: A*, Vol. 541, pp. 181-189. https://doi.org/10.1016/j.msea.2012.02.019

[47] MITCHELL, E.B., LUCON, E., COLLINS, L.E., CLARKE, A.J., CLARKE, K.D. (2021). Microstructure and thickness effects on impact behavior and separation formation in X70 pipeline steel. In: *The Journal of the Minerals, Metals & Materials Society*, Vol. 73, pp. 1966-1977. https://doi.org/10.1007/s11837-021-04562-9

[48] SCHOLL, S., SCHNEIDER, A., SCHWINN, V. (2022). Significance of separations occurring in mechanical testing of thermomechanical rolled pipeline steels. In: *Journal of Pipeline Science and Engineering*, Vol. 2, pp. 100070. https://doi.org/10.1016/j.jpse.2022.100070

[49] CHO, Y.H., LEE, J., CHOO, W.Y., KANG, J., HAN, H.N. (2022). Effect of separation on the fracture surface of pipeline steels with ferrite-bainite dual phases during drop weight tear test. In: *Metals and Materials International*, Vol. 28, pp. 1340-1348. https://doi.org/10.1007/s12540-021-00999-4.